



This discussion paper is/has been under review for the journal Biogeosciences (BG).  
Please refer to the corresponding final paper in BG if available.

# Modeling the sensitivity of soil mercury storage to climate-induced changes in soil carbon pools

O. Hararuk<sup>1</sup>, D. Obrist<sup>2</sup>, and Y. Luo<sup>1</sup>

<sup>1</sup>Department of Microbiology and Plant Biology, University of Oklahoma, Norman, Oklahoma, USA

<sup>2</sup>Desert Research Institute, Reno, Nevada, USA

Received: 18 May 2012 – Accepted: 25 July 2012 – Published: 23 August 2012

Correspondence to: O. Hararuk (ohararuk@ou.edu)

Published by Copernicus Publications on behalf of the European Geosciences Union.

BGD

9, 11403–11441, 2012

Climate-induced  
changes in soil  
carbon pools

O. Hararuk et al.

Title Page

Abstract

Introduction

Conclusions

References

Tables

Figures

◀

▶

◀

▶

Back

Close

Full Screen / Esc

Printer-friendly Version

Interactive Discussion



## Abstract

Substantial amounts of mercury (Hg) in the terrestrial environment reside in soils and are associated with soil organic carbon (C) pools, where they accumulated due to increased atmospheric deposition due to anthropogenic activities. The purpose of this 5 study was to examine potential sensitivity of surface soil Hg pools to global change variables, particularly affected by predicted changes in soil C pools, in the contiguous US. To investigate, we included a soil Hg component in the Community Land Model based on empirical statistical relationships between soil Hg/C ratios and precipitation, 10 latitude and clay; and subsequently explored the sensitivity of soil C and soil Hg densities (i.e. areal-mass) to climate scenarios in which we altered annual precipitation, carbon dioxide (CO<sub>2</sub>) concentrations, and temperature.

Our model simulations showed that current sequestration of Hg in the contiguous US accounted for 15 230 metric tons of Hg in the top 0–40 cm of soils. In the simulations, these soil Hg pools were most sensitive to changes in precipitation because 15 of strong effects on soil C pools plus a direct effect of precipitation on soil Hg/C ratios. Soil Hg pools were predicted to increase beyond present-day values following an increase in precipitation amounts and decrease following a reduction in precipitation. We found pronounced regional differences in sensitivity of soil Hg to precipitation, which were particularly high along high-precipitation areas along the West and East 20 Coasts. Modeled increases in CO<sub>2</sub> concentrations to 700 ppm stimulated soil C and Hg densities, while increased air temperatures had small negative effects on soil C and Hg. The combined effects of increased CO<sub>2</sub>, increased temperature, and increased or decreased precipitation were strongly governed by precipitation and CO<sub>2</sub> showing pronounced regional patterns. Based on these results, we conclude that the combination 25 of precipitation and CO<sub>2</sub> should be emphasized when assessing how climate-induced changes in soil C may affect sequestration of Hg in soils.

## Climate-induced changes in soil carbon pools

O. Hararuk et al.

[Title Page](#)

[Abstract](#)

[Introduction](#)

[Conclusions](#)

[References](#)

[Tables](#)

[Figures](#)

◀

▶

◀

▶

[Back](#)

[Close](#)

[Full Screen / Esc](#)

[Printer-friendly Version](#)

[Interactive Discussion](#)



# 1 Introduction

Mercury (Hg) is considered a global environmental pollutant and its dominant form in the atmosphere – gaseous elemental Hg – has a long atmospheric residence time (6 to 24 months), allowing for global redistribution (Schroeder and Munthe, 1998; Fitzgerald et al., 1998; Coughenour and Chen, 1997).

Many natural sources exist that emit Hg into the atmosphere – including volcanic sources, biomass burning, and surface evasion – but during the last 150 yr, atmospheric Hg loads are estimated to have increased three-to-five orders of magnitude due to anthropogenic emissions from gold mining, coal burning, waste incineration, and industrial processes (Biester et al., 2003; Fitzgerald et al., 1998; Schuster et al., 2002; Streets et al., 2011). Mercury is of greatest concern when inorganic Hg is methylated and biomagnified through the food chain in aquatic and terrestrial ecosystems (Morel et al., 1998; Gnamuš et al., 2000), posing high exposure to top predators and humans.

Hg loads in remote terrestrial ecosystems are dominated by atmospheric deposition (Fitzgerald et al., 1998), and large pools of past Hg pollution – or “legacy” pollution – reside in surface litter and soil horizons (Grigal, 2003; Obrist et al., 2009). The accumulation of Hg in terrestrial ecosystems is many orders of magnitude larger than atmospheric pools (Obrist, 2007). Fate processes and potential changes in terrestrial Hg storage have important implications for global cycling of Hg, including implications for back-evasion of Hg back to the atmosphere or runoff to aquatic systems (Obrist, 2007; Smith-Downey et al., 2010). For example, bi-directional flux behavior that Hg shows between terrestrial components and the atmosphere (Erickson et al., 2006; Fritsche et al., 2008) is of concern for atmospheric Hg loads (Erickson et al., 2005; Harris et al., 2007; Pokharel and Obrist, 2011; Obrist et al., 2010b). Re-emissions of Hg from terrestrial surfaces – also termed secondary emissions – have the potential to become increasingly important due to a cumulative effect of past and ongoing pollution loads accumulating in surface reservoirs.

## Climate-induced changes in soil carbon pools

O. Hararuk et al.

[Title Page](#)

[Abstract](#)

[Introduction](#)

[Conclusions](#)

[References](#)

[Tables](#)

[Figures](#)

◀

▶

◀

▶

[Back](#)

[Close](#)

[Full Screen / Esc](#)

[Printer-friendly Version](#)

[Interactive Discussion](#)



In terrestrial ecosystems, Hg mainly is bound to organic matter and carbon (C). In general, Hg depth distributions in soils follow those of soil organic matter, with the highest concentrations found in near-surface layers and decreasing concentrations with depth (Aastrup et al., 1991; Andersson, 1979; Meili, 1991; Obrist et al., 2009). Studies also show corresponding spatial distribution patterns of organic matter and Hg in top soils and litter across multiple sites (Grigal, 2003; Skjelberg et al., 2000; Obrist et al., 2009, 2011). For example, Lag and Steinnes (1978) reported positive correlations between organic matter and Hg (with  $r^2$  of 0.58 and 0.55, respectively) content across Eastern and Northern Norway humus layers, and Obrist et al. (2011) showed regressions between soil organic C and Hg content with coefficient of determination,  $r^2$ , up to 47 % across 14 US forest sites.

Given these correlations between organic matter and Hg, we hypothesized that climate-induced changes in terrestrial C pools might have direct implications for Hg sequestered therein (Obrist, 2007). It is well known that soil C is highly sensitive to climate change – including changes in temperature, precipitation, and carbon dioxide (CO<sub>2</sub>) concentrations (Zheng et al., 2009; Reich and Schlesinger, 1992; Jobbágy and Jackson, 2000; Treseder et al., 2003; Natali et al., 2008). Atmospheric CO<sub>2</sub> concentrations have been steadily increasing since 1850 and are now about 100 ppm higher than pre-industrial levels (Wigley, 1983), with recent increases among the strongest observed in historic times (e.g., 0.9 Gt C yr<sup>-1</sup> from 2000 to 2005 compared to 0.8 Gt C yr<sup>-1</sup> from 1990 to 1999; IPCC, 2007). Increases in the greenhouse gas CO<sub>2</sub> are estimated to increase mean global surface temperatures between 1.8 °C to 4 °C by 2100, depending on emission scenarios (IPCC, 2007). Responses of terrestrial C to climate change are complex: first, elevated atmospheric CO<sub>2</sub> concentrations cause “CO<sub>2</sub> fertilization”, stimulating live and dead biomass accrual and sequestering excess C (Luo et al., 2004; Oren et al., 2001; Norby and Iversen, 2006; Ainsworth and Long, 2005); second, warming experiments show that increasing soil temperatures stimulates soil heterotrophic respiration, thereby releasing sequestered C back into the atmosphere and decreasing soil C residence time (Oechel et al., 2000; Rustad et al., 2001; Melillo et

## Climate-induced changes in soil carbon pools

O. Hararuk et al.

[Title Page](#)

[Abstract](#)

[Introduction](#)

[Conclusions](#)

[References](#)

[Tables](#)

[Figures](#)

◀

▶

◀

▶

[Back](#)

[Close](#)

[Full Screen / Esc](#)

[Printer-friendly Version](#)

[Interactive Discussion](#)



## Climate-induced changes in soil carbon pools

O. Hararuk et al.

[Title Page](#)

[Abstract](#)

[Introduction](#)

[Conclusions](#)

[References](#)

[Tables](#)

[Figures](#)

◀

▶

◀

▶

[Back](#)

[Close](#)

[Full Screen / Esc](#)

[Printer-friendly Version](#)

[Interactive Discussion](#)



sensitive to affecting soil Hg sequestration through underlying soil C changes and direct effects of changed environmental conditions. In addition, our model allows evaluation of regional patterns where strongest sensitivity of both soil C and Hg are expected to occur.

## 5 2 Methods

### 2.1 Model implementation to predict present-day and future soil C and Hg densities

Our modeling simulations are based on the Community Land Model, version 3.5 (CLM3.5) (Oleson, 2004; Oleson et al., 2008), which is predominantly used in the Community Earth System Model (CESM) and Community Atmosphere Model (CAM). This model allows assessment of the physical, chemical, and biological processes by which terrestrial ecosystems are affected across a variety of spatial and temporal scales – including solar and long-wave radiation interactions with vegetation canopy and soil, soil and snow hydrology, heat transfer, and other biogeophysical processes. For simulation 10 of biogeochemical processes (i.e., soil C densities), we used the CASA (Carnegie-Ames-Stanford Approach) sub-model, modified for use in global climate models (Randerson et al., 1997). Each model grid cell was divided into five primary land cover types (glacier, lake, wetland, urban, vegetation), and vegetation land cover type was represented by 15 plant functional types – each of which was represented as a fraction 15 of a grid cell inferred from 1 km satellite data (Bonan et al., 2002a, b). CLM-CASA simulates gross primary productivity (GPP) and converts it to net primary productivity (NPP), assuming that plants use 50 % of the newly acquired C for autotrophic respiration. NPP is then partitioned into three live C pools (stems, leaves, and roots) by three 20 coefficients that vary with plant functional type and water availability. In forests, a fraction of NPP is allocated to stems; whereas in grasslands, NPP is partitioned between roots and leaves. If the plant functional type is water-limited at the particular time step, 25

BGD

9, 11403–11441, 2012

Climate-induced changes in soil carbon pools

O. Hararuk et al.

[Title Page](#)

[Abstract](#)

[Introduction](#)

[Conclusions](#)

[References](#)

[Tables](#)

[Figures](#)

◀

▶

◀

▶

[Back](#)

[Close](#)

[Full Screen / Esc](#)

[Printer-friendly Version](#)

[Interactive Discussion](#)



more C is allocated to roots. From the live pools, C transfers to the dead pools: first to litter and eventually to soil pools, respiring CO<sub>2</sub> at each step of the transfer (Eq. 1):

$$\frac{dX(t)}{dt} = -\xi_1(t)\mathbf{ACX}(t) + \xi_2(t)\mathbf{BU}(t) \quad (1)$$

where  $\frac{dX(t)}{dt}$  is change in each C pool at each time step,  $\xi_1(t)$  is the function of the influence of climate on C loss from each pool;  $\mathbf{A}$  is a  $12 \times 12$ -sized matrix of partitioning coefficients between C pools, which includes soil texture and lignin influence on soil decomposition;  $\mathbf{C}$  is the diagonal matrix of baseline C transfer coefficients, or the C loss rate at 25 °C;  $\mathbf{X}(t)$  is a  $12 \times 1$ -sized vector of C pools (three live pools and nine dead pools);  $\xi_2(t)$  is the function of water limitation of NPP partitioning between three live pools;  $\mathbf{B}$  is the vector of the partitioning coefficients of NPP to the three live pools; and  $U(t)$  is NPP.

We first used the CLM-CASA model to simulate soil C distribution in terrestrial ecosystems in the contiguous US. We then added an Hg component (Eq. 2) to the biogeochemistry module of the CLM-CASA model to predict soil Hg densities. Mercury was implemented into the model using observed Hg/C ratios and statistical relationships of Hg/C ratios to latitude, precipitation, and soil texture observed in a field investigation of 14 forest sites across the US (Obrist et al., 2011). Hg levels were calculated based on the following linear multi-regression model:

$$\ln\left(\frac{\text{Hg}}{\text{C}}\right) = 0.066 \cdot \text{Lat} + 0.001 \cdot P + 0.05 \cdot \text{Clay} + 3.059041 \quad (2)$$

$$\text{Hg} = \frac{\left(\text{C} \cdot \frac{\text{Hg}}{\text{C}}\right)}{1000000} \quad (3)$$

where  $\frac{\text{Hg}}{\text{C}}$  is an Hg/C ratio ( $\mu\text{g g}^{-1}$ ), "Lat" is latitude (degrees),  $P$  is annual precipitation (mm), "Clay" is clay content in the soil (%), Hg is Hg density in the top 40 cm of soil

[Title Page](#)

[Abstract](#)

[Introduction](#)

[Conclusions](#)

[References](#)

[Tables](#)

[Figures](#)

◀

▶

◀

▶

[Back](#)

[Close](#)

[Full Screen / Esc](#)

[Printer-friendly Version](#)

[Interactive Discussion](#)



( $\mu\text{g g}^{-1}$ ), and  $C$  is organic C density in the top 40 cm of soil ( $\text{g m}^{-2}$ ). This linear multi-regression model for Hg/C ratios showed a coefficient of determination,  $r^2$ , of 50 %. In Obrist et al. (2011), we found that a multi-regression model with Hg concentration (as opposed to Hg/C ratios) would increase  $r^2$  from 0.50 to 0.87; but we chose to use Hg/C ratios in our model because terrestrial C models generally predict soil C densities (in  $\text{g m}^{-2}$ ) rather than C concentrations, and conversion of C densities to C concentrations would require soil bulk densities which are not spatially available for the CLM-CASA model.

To examine the effects of changing temperature, precipitation, and atmospheric  $\text{CO}_2$ , we first ran the model (or spun-up) until equilibrium state was reached (i.e., when annual net ecosystem C exchange was close to zero; Fig. 1). The model was spun up for 4000 yr until equilibrium state was reached according to the method described in the Carbon-Land Model Inter-comparison Project (C-LAMP) by (Randerson et al., 2009). The model was cycled through atmospheric forcing data (three-hourly temperature, wind speed, precipitation, photosynthetically active radiation, humidity, and surface pressure) (Qian, 2006) using climate data averaged for the period from 1948 to 1978 in the US.

## 2.2 Simulation scenarios to assess sensitivities of soil C and Hg densities to global change factors

To simulate the sensitivity of soil C and Hg densities to various climate factors, we implemented three levels of treatments for each variable: 280, 390, and 700 ppm for  $\text{CO}_2$ ; +0 %, +50 %, and -50 % from present-day levels for precipitation; and +0  $^{\circ}\text{C}$ , +3  $^{\circ}\text{C}$ , and +6  $^{\circ}\text{C}$  increase in mean annual temperature compared to present-day levels (Fig. 1). The  $\text{CO}_2$  and temperature changes were based on the changes projected by IPCC (IPCC, 2007). Ensemble model projections for the mean global precipitation range from 2.8 % to 6.6 % increase (Emori and Brown, 2005). However, precipitation change is highly variable on the regional scale; for instance, in Central USA

## Climate-induced changes in soil carbon pools

O. Hararuk et al.

[Title Page](#)

[Abstract](#)

[Introduction](#)

[Conclusions](#)

[References](#)

[Tables](#)

[Figures](#)

◀

▶

◀

▶

[Back](#)

[Close](#)

[Full Screen / Esc](#)

[Printer-friendly Version](#)

[Interactive Discussion](#)



## Climate-induced changes in soil carbon pools

O. Hararuk et al.

[Title Page](#)

[Abstract](#)

[Introduction](#)

[Conclusions](#)

[References](#)

[Tables](#)

[Figures](#)

[◀](#)

[▶](#)

[◀](#)

[▶](#)

[Back](#)

[Close](#)

[Full Screen / Esc](#)

[Printer-friendly Version](#)

[Interactive Discussion](#)



precipitation amount is projected to decrease by up to 25 % compared to the present-day levels, and in Northeast and Northwest of USA precipitation is anticipated to increase by about 10 % (Emori and Brown, 2005). However, Zhang et al. (2007) showed that models do not represent regional variability well. For instance, models underpredicted historical 75-yr trend in precipitation by 300 % along 30° N latitude, by 176 % along 40° N, and by 900 % along 50° N (Zhang et al., 2007). Hence, we decided to change precipitation uniformly across USA by higher fractions than the ones predicted by Emori and Brown (2005).

To obtain the atmospheric CO<sub>2</sub> level of 390 ppm, we gradually increased CO<sub>2</sub> concentrations for 300 yr to reach 390 ppm. We then kept it constant for the next 100 yr of the model run. To obtain CO<sub>2</sub> levels of 700 ppm, we gradually increased CO<sub>2</sub> concentrations to 390 ppm for 300 yr. We then gradually increased the CO<sub>2</sub> concentration for 100 yr until it reached 700 ppm by the end of 2100. We increased the mean annual temperature and precipitation amount during these last 100 yr of model runs for all runs.

### 2.3 Calculating combined effects of changes in CO<sub>2</sub>, temperature, and precipitation

We calculated six main effects representing impacts of individual climate change variables, 12 two-way interactive effects (data not shown, but used to calculate three-way effects), and eight three-way interactive effects combining changes in CO<sub>2</sub> levels, temperature, and precipitation. To calculate main and interactive effects, we used the method described earlier by Luo et al. (2008). We calculated the main effect of an environmental factor by averaging nine simple effects of each environmental factor. For example, the effect of reduced precipitation under unchanged temperature and CO<sub>2</sub> concentration was calculated as follows:

$$P_{-50\%} = (C_{280}T_{+0}P_{-50\%} - C_{280}T_{+0}P_{+0\%}) \quad (4)$$

## Climate-induced changes in soil carbon pools

O. Hararuk et al.

[Title Page](#)

[Abstract](#)

[Introduction](#)

[Conclusions](#)

[References](#)

[Tables](#)

[Figures](#)

[◀](#)

[▶](#)

[◀](#)

[▶](#)

[Back](#)

[Close](#)

[Full Screen / Esc](#)

[Printer-friendly Version](#)

[Interactive Discussion](#)



where  $C_{280}T_{+0}P_{-50\%}$  represents the model run with unchanged temperature and CO<sub>2</sub> concentrations but with reduced precipitation. In similar ways, we calculated eight other simple effects of decreased precipitation using all combinations of temperature and precipitation conditions, then averaged the effects for a main effect for reduced precipitation conditions. The same operation was repeated for all other five main effects.

Two-way interactive effects were calculated by averaging three simple effects of two variables altered simultaneously, and subtracting the main effects of the corresponding variables. The simple effects were calculated as follows:

$$P_{-50\%} \times T_{+31} = (C_{280}T_{+3}P_{-50\%} - C_{280}T_{+0}P_{+0\%}) - P_{-50\%} - T_{+3} \quad (5)$$

where  $P_{-50\%} \times T_{+31}$  is the simple effect of simultaneously reduced precipitation and increased temperature;  $C_{280}T_{+3}P_{-50\%}$  is the model run with increased temperature (by 3 °C), decreased precipitation, and unchanged CO<sub>2</sub>;  $C_{280}T_{+0}P_{+0\%}$  is the control run,  $P_{-50\%}$  is the main effect of reduced precipitation, and  $T_{+3}$  is the main effect of the 3 °C temperature increase. The same calculation was performed for two other simple effects for reduced precipitation and increased temperature. We then averaged the simple effects and subtracted from the average the main effects of reduced precipitation and increased temperature. We completed the same calculation for 11 other two-way interactive effects.

Three-way interactive effects were calculated by subtracting the main and two-way interactive effects from model runs with simultaneously altered CO<sub>2</sub>, temperature, and precipitation:

$$P_{-50\%} \times C_{+110} \times T_{+3} = (C_{+110}T_{+3}P_{-50\%} - C_{280}T_{+0}P_{+0\%}) - P_{-50\%} - T_{+3} - C_{+110} - P_{-50\%} \times C_{+110} - C_{+110} \times T_{+3} - P_{-50\%} \times T_{+3} \quad (6)$$

where  $P_{-50\%} \times C_{+110} \times T_{+3}$  is the magnitude of the three-way interactive effect between reduced precipitation, increased CO<sub>2</sub>, and increased temperature;  $C_{+110}T_{+3}P_{-50\%}$  is the model run in which we simultaneously decreased the precipitation amount while increasing CO<sub>2</sub> and temperature;  $P_{-50\%}$ ,  $T_{+3}$ , and  $C_{+110}$  are the main effects of decreased precipitation, temperature increased by 3 °C, and CO<sub>2</sub> increased by 110 ppm;

$P_{-50\%} \times C_{+110}$ ,  $C_{+110} \times T_{+3}$ , and  $P_{-50\%} \times T_{+3}$  are two-way interactive effects of reduced precipitation and increased  $\text{CO}_2$ , increased  $\text{CO}_2$  and increased temperature, and decreased precipitation and increased temperature.

BGD

9, 11403–11441, 2012

To assess the strength of the two-way and three-way interactive effects, we calculated their strength relative to the averaged magnitude of the main corresponding effects. The relative strength for the two-way interactive effect was calculated as follows:

$$I_2 = \frac{2 \times T_{+3} \times P_{-50\%}}{|P_{-50\%}| + |T_{+3}|} \quad (7)$$

where  $I_2$  is a relative strength of the two-way interaction,  $T_{+3} \times P_{-50\%}$  is the magnitude of the two-way interactive effect of increased temperature and reduced precipitation,  $P_{-50\%}$  is the main effect of reduced precipitation, and  $T_{+3}$  is the main effect of increased temperature. The three-way interactive effect was calculated as follows:

$$I_2 = \frac{2 \times T_{+3} \times P_{-50\%} \times C_{+110}}{|P_{-50\%}| + |T_{+3}| + |C_{+110}|} \quad (8)$$

where  $T_{+3} \times P_{-50\%} \times C_{+110}$  is the magnitude of the three-way interactive effect between increased temperature, reduced temperature, and increased  $\text{CO}_2$ ; and  $C_{+110}$  is the main effect of increased  $\text{CO}_2$ .

The effects of the combined environmental variables for each run were calculated as the sum of all corresponding main and interactive effects.

### 3 Results and discussion

#### 20 3.1 Model evaluation and comparisons to observations and other model data

Figure 2a and b show present-day soil C and Hg densities for the top 40 cm of soils as predicted by the model for the contiguous US. Top soil C under present-day  $\text{CO}_2$

Title Page

Abstract

Introduction

Conclusions

References

Tables

Figures

◀

▶

◀

▶

Back

Close

Full Screen / Esc

Printer-friendly Version

Interactive Discussion



concentrations, temperature, and precipitation ranged from 0.78 to 29.34 kg m<sup>-2</sup>. Spatial heterogeneity of soil C is mainly controlled by NPP, soil residence time, and human disturbance (e.g., conversion of grasslands to croplands) (Zhou and Luo, 2008; Guo et al., 2006). Both NPP and soil C residence time depend on temperature and precipitation. Apart from climate, soil residence times depend on soil texture and lignin content (Parton et al., 1987). If soil C is rich in lignin, the decomposition rate of soil C will be slower, increasing its residence time; soils higher in clay content tend to stabilize more C, increasing soil C residence time. Previous study of soil C distribution in the conterminous US revealed that apart from land use change, precipitation has the most evident positive effect on soil C; and, within narrow precipitation ranges, temperature controls soil C stocks and soil C decreases non-linearly with increase in temperature (Guo and Gifford, 2002). We were able to duplicate general patterns of topsoil C distribution (Fig. 2a) in agreement with observational (Group, 2000; Guo et al., 2006) and modeling studies (Randerson et al., 2009). For example, we predicted that (i) lowest soil C densities would occur in the arid West and Midwest, caused by a combination of unfavorable climatic conditions for plant productivity (i.e., aridity) and land use (extensive areas occupied by croplands); (ii) higher C stocks in the forested zones of the northwestern, northeastern, and southeastern US caused by higher plant productivity and higher annual rainfall; and (iii) latitudinal increases in soil C along the East and West Coasts in accordance with predicted temperature effects.

In Fig. 2c, we compare C densities obtained by our simulation with observed soil C densities. For observed C, we used the IGBP-DIS gridded soil C data set with 5 × 5 arc minute resolution (Group, 2000). We found a good regression coefficient,  $r^2$ , between these two data sets of 0.49, indicating that our model simulation agreed relatively well with the observed data in regard to spatial patterns predicted for soil C distribution in the US. We found, however, that our modeling predictions underestimated soil C densities compared to the data from IGBP-DIS by approximately 60 %, and corrected modeled data for this underprediction. Discrepancies between observed values and model predictions can be explained by potential underestimation of soil C residence times; for

## Climate-induced changes in soil carbon pools

O. Hararuk et al.

[Title Page](#)

[Abstract](#)

[Introduction](#)

[Conclusions](#)

[References](#)

[Tables](#)

[Figures](#)

◀

▶

◀

▶

[Back](#)

[Close](#)

[Full Screen / Esc](#)

[Printer-friendly Version](#)

[Interactive Discussion](#)



instance, the residence times for slow, passive, and whole soil C pools produced by the CLM-CASA model for the Duke Forest were 9, 88, and 10 yr, respectively; whereas Luo et al. (2001b) reported 31, 885, and 47 yr for the same C pools. The cause for such underprediction may lie in underestimation of the lignin effect on soil residence times by the model, as well as underprediction of the effect of soil texture on soil C residence times (Parton et al., 1987).

Figure 2b shows predicted soil Hg densities for the continental US, and Fig. 2d shows predicted soil Hg densities and observed Hg densities at 14 field observation sites plus additional published data found in sites across the US (Stamenkovic et al., 2008; Ma et al., 1997; Obrist et al., 2011; Amirbahman et al., 2004; Cohen et al., 2009; Demers et al., 2007; Dicosti et al., 2006; Dreher and Follmer, 2004; Grigal, 2003; Engle et al., 2006; Nater and Grigal, 1992; Natali et al., 2008). On average, observed and predicted soil Hg densities were within 15.6 % of each other ( $r = 0.47$ ,  $p = 0.024$ ). Best agreement was generally observed in sites located in Florida, Washington, California, Nevada, North Carolina, and Tennessee, while Hg stocks were under and overpredicted at sites in Maine, New Hampshire, and the Great Lakes region. Clearly, inaccuracies in predicted soil C densities directly affect predicted Hg densities because soil C density forms the underlying variability for Hg density predictions that are based on Hg/C values. Furthermore, the coefficient of determination of the multiple linear regression model for Hg/C ratios used to estimate Hg distribution is 0.50; hence, significant variability in the distribution of soil Hg must be explained by factors that are not included in our model. Many factors, including biogeochemical processes, spatial/temporal aspects of field sampling, regional pollution effects, and others can explain the discrepancies between field observations and the model.

Spatial distribution patterns of model predictions generally agreed with those of soil Hg densities observed across field sites (i.e., Fig. 2d). Distribution of soil Hg densities also agreed well with observed and interpolated distribution of Hg concentrations, as extrapolated in a previous manuscript (Obrist et al., 2011). In that study, top soil Hg concentrations were extrapolated to the contiguous US based on a multi-regression

## Climate-induced changes in soil carbon pools

O. Hararuk et al.

[Title Page](#)

[Abstract](#)

[Introduction](#)

[Conclusions](#)

[References](#)

[Tables](#)

[Figures](#)

◀

▶

◀

▶

[Back](#)

[Close](#)

[Full Screen / Esc](#)

[Printer-friendly Version](#)

[Interactive Discussion](#)



**Climate-induced changes in soil carbon pools**

O. Hararuk et al.

[Title Page](#)[Abstract](#)[Introduction](#)[Conclusions](#)[References](#)[Tables](#)[Figures](#)[◀](#)[▶](#)[◀](#)[▶](#)[Back](#)[Close](#)[Full Screen / Esc](#)[Printer-friendly Version](#)[Interactive Discussion](#)

model with an  $r^2$  of 0.88; these results showed a clear trend of increasing Hg concentrations with increasing latitude and highest Hg concentrations in the northeastern and northwestern US, in accordance with the predicted soil Hg density distributions in Fig. 2b: highest soil Hg densities were found in two sites located in Washington State and a site in Maine, while southwestern and midwestern pool sizes showed among the lowest soil Hg densities of all sites. Total soil Hg mass (0–40 cm depth) estimated based on these model results accounted for 15 230 metric tons of Hg across the US.

In Fig. 3, we compared sensitivity of soil C densities to variation in global change variables of our model simulations (as presented in Figs. 4 to 6) and those reported by Treseder et al. (2003), Natali et al. (2008), Pepper et al. (2005), Coughenour and Chen (1997), Cox et al. (2000), Cramer et al. (2001), Lichter et al. (2005), Lu et al. (2008), Shen et al. (2009), Talmon et al. (2011), and Wang et al. (2011). Specifically, we assessed the sensitivity of soil C densities to individual climate change variables, including increases in temperature,  $\text{CO}_2$ , changes in precipitation patterns, and combinations of these factors. We found, in general, good agreement in the direction of the soil C density changes: 91 % of analyzed data point pairs agreed in the direction of soil C density changes in the models; in only about 9 % of predictions did we find that our model predicted different direction of soil C changes. For example, when comparing effects of  $\text{CO}_2$  on soil C, we found relatively good correlation of predicted effects ( $r = 0.5$ ,  $p = 0.04$ ). Most models, including ours, predicted soil C to increase significantly under elevated  $\text{CO}_2$ , with the exception of the DayCent model (Pepper et al., 2005), which projected a decrease in soil C under elevated  $\text{CO}_2$  due to nitrogen limitation. Without the DayCent model data, the coefficient of determinations between ours and other simulations increased further ( $r = 0.6$ ,  $p = 0.018$ ).

Still, there are some discrepancies in regard to the magnitude of predicted soil C changes between our model and other model predictions; in particular, our simulations generally overpredicted effects of  $\text{CO}_2$  increases and temperature plus  $\text{CO}_2$  increases on soil C content compared to other simulations. Our CLM-CASA model simulations on average overpredicted  $\text{CO}_2$  effects by 8.4 % compared to other model simulations;

## Climate-induced changes in soil carbon pools

O. Hararuk et al.

[Title Page](#)

[Abstract](#)

[Introduction](#)

[Conclusions](#)

[References](#)

[Tables](#)

[Figures](#)

◀

▶

◀

▶

[Back](#)

[Close](#)

[Full Screen / Esc](#)

[Printer-friendly Version](#)

[Interactive Discussion](#)



without the DayCent model data, however, these differences in CO<sub>2</sub> effects reduced to 5.7 %. In addition, our model underpredicted the combined effects of changes in temperature, CO<sub>2</sub>, and precipitation. Such differences may have been due to use of different climate change scenarios: we compared model outputs from the simulation scenarios that differed from ours by 1 °C in temperature, up to 100 ppm in CO<sub>2</sub>, and up to 20 % in precipitation. Also, differences in model structures may have caused discrepancies in the predicted climate effect on soil C, including parameterizations of water and nutrient limitations.

### 3.2 Sensitivity of soil C and Hg densities to individual climate change variables

#### 10 3.2.1 Sensitivity to change in air temperature

Increases in air temperature (top panel) caused consistent decreases in soil C densities across all regions of the US; such responses to temperature have been well characterized and attributed to more significant stimulation of heterotrophic respiration with increasing temperature (Wu et al., 2011; Rustad et al., 2001; Zheng et al., 2009; Reich and Schlesinger, 1992) compared to temperature-induced stimulation of NPP (Rustad et al., 2001). The average C loss predicted by our model for a temperature increase of 6 °C is estimated at 10 % and is similar to six models that predicted an average soil C decrease of 11 % when temperature was increased by 5 °C (Cramer et al., 2001). Regional differences for soil C densities show that most pronounced losses are expected in the central and southeastern US (between 20 and 30 %). Observational studies by Guo et al. (2006) reveal a polynomial relationship between soil C and temperature in high precipitation forests, such that soil C increases upon temperature increases from 8 °C to 11 °C but not (or slightly decrease) upon temperature increases from 8 °C to 15 °C. Our spatial predictions agree with the above patterns, such that we observe the very small decreases (and slight increases) in soil C densities in the Northeast and Northwest, while more southern sites showed pronounced losses of soil C densities. Guo et al. (2006) also indicated pronounced soil C losses (17 to 32 %) with temperature

increases of 3 °C and 6 °C in a region with 1000–1150 mm precipitation ranges. Such precipitation corresponds, for example, to southeastern forests where our simulations predicted significant decreases in soil C as well. Guo et al. (2006) also report that drier grassland areas are more sensitive to temperature increase than forest areas with similar precipitation or forest areas with higher precipitation. In Fig. 4a, we observe that grasslands (e.g., in Texas, Kansas, Nebraska, and South Dakota) tend to lose more C than forested areas (e.g., in Idaho, Washington, Maine) under temperature increases.

Based on the multi-linear model used for Hg soil density prediction, effects of temperature on soil C densities will directly and linearly feedback to soil Hg densities because Hg/C ratios are directly multiplied by underlying soil C densities and because temperature has no direct statistical relationships with Hg/C ratios (as opposed to precipitation, see below). Hence, our sensitivity analyses predicted identical changes in soil Hg compared to soil C, with losses averaging 4.7 % for a 3 °C increase in mean annual temperatures and 10 % with a 6 °C increase across the continent. Responses of soil Hg densities are predicted to be highly regional and are expected to follow the spatial patterns discussed above in regards to soil C densities: the strongest responses on soil Hg densities are expected in the south and central US where our model predicts losses in soil Hg densities up to 30 % of present-day levels. Further losses would be expected in the southern US and Great Plains while low sensitivity to air temperature is expected in the northeastern and northwestern US where soil C densities are not particularly sensitive to changes in temperature.

Our statistical modeling approach does not allow for characterization of underlying processes that lead to changes in soil Hg densities, but it seems reasonable to assume that areas showing pronounced changes in soil C are those that might be most sensitive to changes in Hg that are generally sequestered in such C pools. Hence, it is likely that soil Hg pools most sensitive to temperature changes are those located in the central and southern US, while northwest and northeast areas show little sensitivity. We must, however, put strong limitations on the magnitude of predicted changes in soil Hg densities because using direct (i.e., linear) relationships between soil Hg and C

## Climate-induced changes in soil carbon pools

O. Hararuk et al.

[Title Page](#)

[Abstract](#)

[Introduction](#)

[Conclusions](#)

[References](#)

[Tables](#)

[Figures](#)

◀

▶

◀

▶

[Back](#)

[Close](#)

[Full Screen / Esc](#)

[Printer-friendly Version](#)

[Interactive Discussion](#)



changes that result from our model implementation are highly unlikely in reality. For example, linear responses between Hg and C changes might be expected upon complete loss of both Hg and organic C pools (e.g., that may occur in surface organic horizons during wildfires) where significant Hg losses have in fact been observed (Artaxo et al., 2000; Brunke et al., 2001; Friedli et al., 2001; Sigler et al., 2003; Turetsky et al., 2006; Obrist et al., 2008). In contrast, however, the few experimental studies that correspondingly measured the fate of Hg upon C mineralization indicate that only a small fraction of Hg may be subject to volatilization losses upon evasion of CO<sub>2</sub> (Fritsche et al., 2008; Obrist et al., 2010b), which would indicate a much smaller magnitude of soil Hg losses compared to that of C. The biogeochemistry of terrestrial Hg is very complex, including various deposition and emission pathways (e.g., Graydon et al., 2008a; Gustin et al., 2008), redox transformations between volatile and non-volatile Hg forms (Lalonde et al., 2001; Obrist et al., 2010a), and methylation and demethylation processes (Ullrich et al., 2001). The statistical approach used in this study does not allow simulating individual biogeochemical processes, and clearly the quantitative response of Hg upon changes in soil C will depend on these underlying processes and need to be addressed by further experimental studies.

### 3.2.2 Sensitivity to precipitation changes

Of the three variables tested, we found that changes in precipitation had the highest sensitivity for soil Hg densities (note different scales in Fig. 4). Unlike effects of temperature, our model predicted that precipitation affects soil Hg and soil C densities (Fig. 4c and d) in different ways. This is because changes in precipitation patterns affect underlying soil C densities and also Hg/C ratios used to calculate soil Hg densities. For soil C densities, changes in precipitation patterns are highly regional; a 50 % decrease in precipitation, for example, would decrease soil C densities – up to 33 % – in the central part of the US and up to 18 % in Florida; soil C densities, alternatively, remained relatively unchanged in many West Coast regions with precipitation change; soil C densities even would decrease slightly in the Northeast with increased precipitation. If

## Climate-induced changes in soil carbon pools

O. Hararuk et al.

[Title Page](#)

[Abstract](#)

[Introduction](#)

[Conclusions](#)

[References](#)

[Tables](#)

[Figures](#)

◀

▶

◀

▶

[Back](#)

[Close](#)

[Full Screen / Esc](#)

[Printer-friendly Version](#)

[Interactive Discussion](#)



we divided regions by precipitation gradients, we generally observed that with precipitation below 850 mm per year, a 50 % decrease in precipitation would lead to strong decreases in soil C (34 % on average) and, hence, these decreases have greatest implications across the arid western and midwestern US.

5 We observed the same patterns under increased precipitation. For instance, more humic areas (such as coastal areas and southeastern US) showed less sensitivity to precipitation changes. Such patterns in soil C change are supported by Guo et al. (2006), who reported an increase in soil C, on average by 23 %, with a 50 % increase in precipitation if the original annual precipitation were up to 700 mm. Altered precipitation influences both NPP and soil respiration (Wu et al., 2011; Huxman et al., 2004).  
10 Soil respiration generally is more sensitive to precipitation in dry areas compared to wet areas (Wu et al., 2011), thereby increasing sensitivity to respective changes in arid regions. NPP in areas with high rainfall also is less sensitive to additional precipitation compared to arid regions (Huxman et al., 2004). Hence, in mesic regions, additional precipitation will cause little to no change in NPP and little increase in soil respiration;  
15 in dry regions, additional precipitation particularly will stimulate NPP – but less so heterotrophic respiration – resulting in net gains in C accumulation (Wu et al., 2011). Drought conditions will cause a disproportionately large C imbalance in arid ecosystems – despite relatively uniform water use efficiency – compared to mesic regions due  
20 to strong sensitivity of soil respiration to reduced rainfall (Wu et al., 2011; Huxman et al., 2004).

The sensitivity of soil Hg densities to precipitation is spatially different compared to that of soil C densities, which is due to the additional effect that precipitation has on Hg/C ratios. We previously observed that annual precipitation is positively correlated to soil Hg concentrations across US forests (Obrist et al., 2011), and the multi-regression equation above (Eq. 2) accounts for this influence also in regard to Hg/C ratios. Hence, soil Hg densities are expected to decrease under reduced precipitation more than would be expected purely due to changes in soil C, and increase more than soil C under increased precipitation scenarios. Assuming linearity between soil C and

## Climate-induced changes in soil carbon pools

O. Hararuk et al.

[Title Page](#)

[Abstract](#)

[Introduction](#)

[Conclusions](#)

[References](#)

[Tables](#)

[Figures](#)

◀

▶

◀

▶

[Back](#)

[Close](#)

[Full Screen / Esc](#)

[Printer-friendly Version](#)

[Interactive Discussion](#)



soil Hg changes, we found that effects of increased precipitation on Hg/C ratios alone accounted for about 53 % of the changes in soil Hg densities, which in reality is likely even higher. Our model sensitivity study indicated that sensitivity of soil Hg changes follows precipitation gradients across the US. For example, assuming linearity between 5 soil C and Hg changes, a 50 % decrease in annual precipitation would decrease Hg stocks by 10 % of present day values in southern California and Arizona but would be much stronger (up to 75 %) in the Northwest as well as along the US East Coast. Further, lower sensitivities to changes in precipitation are predicted to occur in the arid intermountain west, while sensitivities increase gradually towards the East Coast and 10 were particularly high in the eastern and southeastern US.

Aside from the direct effects of soil C on soil Hg densities discussed above, a variety of other processes could explain responses of Hg concentrations and Hg/C ratios to changes in precipitation. For example, precipitation amounts may directly lead to changes in wet deposition loads (NADP, 2011) leading to changes in soil Hg densities 15 (although such effects may be highly non-linear due to “washout” effects (Lamborg et al., 1995; Landis et al., 2002; Lyman and Gustin, 2008; Mason et al., 1997; Faïn et al., 2011). Further, correlations between annual precipitation and soil Hg may be caused by canopy wash-off and throughfall deposition which in forest ecosystems is a significant deposition flux (Demers et al., 2007; Rea et al., 1996; Graydon et al., 2008b), and such 20 deposition loads likely would be efficiently retained in ecosystems (e.g., soils generally retain more than 90 % of Hg deposited with rainfall, Erickson et al., 2005; Harris et al., 2007; Graydon et al., 2009; Hintelmann et al., 2002). Other reasons for effects of precipitation on soil Hg storage are different representations of biomes and soil types in different climate zones.

### 25 3.2.3 Sensitivity to changes in CO<sub>2</sub> concentrations

Increased CO<sub>2</sub> concentrations showed the second highest sensitivity on soil Hg densities. As with effects of temperature, changes in CO<sub>2</sub> levels only affect soil Hg densities through changes in underlying soil C pools in our model; hence, spatial responses

## Climate-induced changes in soil carbon pools

O. Hararuk et al.

[Title Page](#)

[Abstract](#)

[Introduction](#)

[Conclusions](#)

[References](#)

[Tables](#)

[Figures](#)

◀

▶

◀

▶

[Back](#)

[Close](#)

[Full Screen / Esc](#)

[Printer-friendly Version](#)

[Interactive Discussion](#)



to  $\text{CO}_2$  concentration changes are equivalent for soil Hg and C, and the patterns described below hence apply for both soil C and Hg densities. When we increased  $\text{CO}_2$  by 110 ppm from 280 ppm, soil C and Hg densities increased by up to 22 %, with the most responsive areas located in water-limited western lands. When  $\text{CO}_2$  levels were increased by 420 ppm from 280 ppm, soil C and Hg densities increased by up to 50 %. Many studies are available on effects of  $\text{CO}_2$  concentration on terrestrial C; in general, studies show that increased  $\text{CO}_2$  leads to a fertilization effect (Ainsworth and Long, 2005; Norby et al., 2005). Additional  $\text{CO}_2$  leads to increased water use efficiency (Eamus, 1991), plant productivity (De Graaff et al., 2006), plant light-use efficiency (Kubiske and Pregitzer, 1996), and generally also to increased tissue C/N ratios (De Graaff et al., 2006; Luo et al., 2006). Soil C tends to increase in grasslands (10 %) more than in forests (6 %), with a  $\text{CO}_2$  increase to 550 ppm (Luo et al., 2006). These patterns of expected changes in soil C and Hg densities to  $\text{CO}_2$  increases are reflected in our predicted sensitivity maps: for example, the Great Plains show a higher sensitivity to changes in  $\text{CO}_2$  concentrations as compared to northwestern and northeastern forests; the arid intermountain west and the southwestern US shows strong sensitivities of soil C density; and smaller changes are expected to occur along coastal areas and in the southeastern US. Changes in soil C densities are mainly due to stimulation of NPP (i.e.,  $\text{CO}_2$  fertilization effect), as evident by predicted whole plant C increases for most biomes under increasing  $\text{CO}_2$ ; through time, however, progressive nitrogen limitation decreases the response of plant productivity to  $\text{CO}_2$  increases in nutrient poor areas (Oren et al., 2001; Luo et al., 2004; Norby and Iversen, 2006). Although some studies indicate an increase in soil respiration with elevated  $\text{CO}_2$ , carbon dioxide has no stimulation effect on cumulative soil respiration during the long-term (Bader and Körner, 2010; Johnson et al., 2001; Tingey et al., 2006).

Two studies using Free-Air- $\text{CO}_2$ -Enrichment (FACE) experiments showed that a  $\text{CO}_2$  increase from 393 ppm to 549 ppm at the Oak Ridge FACE site increased soil Hg content by 33 %; an increase in  $\text{CO}_2$  from 382 ppm to 582 ppm at the Duke FACE site increased soil Hg content by 21 % (Natali et al., 2008). These soil Hg increases were

## Climate-induced changes in soil carbon pools

O. Hararuk et al.

[Title Page](#)

[Abstract](#)

[Introduction](#)

[Conclusions](#)

[References](#)

[Tables](#)

[Figures](#)

◀

▶

◀

▶

[Back](#)

[Close](#)

[Full Screen / Esc](#)

[Printer-friendly Version](#)

[Interactive Discussion](#)



preliminarily attributed to corresponding increases in top soil organic C content, suggesting that changes in soil C may directly cause changes in soil Hg. Effects of CO<sub>2</sub> on Hg accumulation, however, may in fact not be limited to changes in underlying soil C densities; Millhollen et al. (2006) showed that plant exposure to elevated CO<sub>2</sub> led to lower foliar Hg concentrations in plants; they also suggested that leaf Hg uptake is controlled by leaf physiological processes, including stomatal conductance which is typically reduced under elevated CO<sub>2</sub>. Natali et al. (2008) also found slightly lower foliar Hg concentrations in elevated CO<sub>2</sub> treatments, but the differences were not significant. Further studies are needed to assess additional effects that changes in CO<sub>2</sub> concentrations may have on Hg cycling to accurately assess effects of global change.

### 3.3 Combined effects of climate-change variables on soil C and Hg densities

Climate change factors are not purely additive but can show strong interactive effects between factors, which affects calculation of the combined effects of changes in temperature, precipitation, and CO<sub>2</sub> concentrations. Luo et al. (2008) found that the most significant interactive effects occurred between CO<sub>2</sub> and precipitation, and we found similar model simulation results. For example, interactive effects between changes in precipitation and CO<sub>2</sub> can be expected (as discussed in Sect. 3.2.3) because the response of change in CO<sub>2</sub> is highly dependent on soil water availability across different US regions. Hence, the response of CO<sub>2</sub> is highly dependent on soil water status, and any combination of changes in precipitation and CO<sub>2</sub> will show interactive effects on the predicted sensitivity of soil C and soil Hg densities. We found that other combinations of climate variables (such as temperature and precipitation) had relatively minor interactive effects; for these combinations, the response to climate variables is close to the additive effect of individual global climate variables.

Figure 5 shows the combined sensitivity of the three tested climate variables on soil C and soil Hg densities. In general, we found similar responses to changes in environmental variables as highlighted above. Since the strongest sensitivity for soil C and Hg densities was predicted to occur in response to changes in precipitation (Sect. 3.2.2),

## Climate-induced changes in soil carbon pools

O. Hararuk et al.

[Title Page](#)

[Abstract](#)

[Introduction](#)

[Conclusions](#)

[References](#)

[Tables](#)

[Figures](#)

◀

▶

◀

▶

[Back](#)

[Close](#)

[Full Screen / Esc](#)

[Printer-friendly Version](#)

[Interactive Discussion](#)



changes in precipitation also mainly drove the changes when all three variables were combined. These interactive effects also showed that soil C and Hg densities were least sensitive to temperature changes compared to CO<sub>2</sub> and precipitation changes; hence, we found relatively small additional differences in precipitation changes compared to the greater effects of CO<sub>2</sub>. Figure 5 highlights the sensitivity of soil C and soil Hg densities, suggesting it may be most important to focus on effects of CO<sub>2</sub> and precipitation and their combinations, as these show greatest sensitivity and strong interactive effects. This is in agreement with the results of both modeling studies and meta-analyses, focusing on the effects of precipitation and CO<sub>2</sub> on the C cycle (Luo et al., 2008; Housman et al., 2006; De Graaff et al., 2006; Natali et al., 2008).

## 4 Conclusions

In conclusion, our study assessed potential sensitivity of changes in climate variables on soil C density distribution across the US, which we used to assess how this might affect soil Hg pools that show correlations to soil C distributions. It is important to note that our study was not intended to simulate process-driven and biogeochemical changes in Hg cycling under climate change but rather is based on statistical relationships of Hg to soil C and other environmental variables observed in the field under present-day conditions.

Our study indicated a high sensitivity (on average +16 % of present-day levels) with a CO<sub>2</sub> increase from 390 ppm to 700 ppm for soil C densities, which is likely to show strong potential for significant changes in soil Hg due to their association. This result is in agreement with field observations showing that soil Hg is sensitive to CO<sub>2</sub>-induced increases in soil C pools in two experimental forest CO<sub>2</sub> manipulation studies (Natali et al., 2008). Unlike effects of CO<sub>2</sub>, changes in precipitation patterns were anticipated to show dissimilar spatial changes for soil C and soil Hg, in particular because precipitation was expected to affect both soil C and soil Hg/C levels. Both soil C and soil Hg were only moderately sensitive to increases in temperature, and the resulting regional

## Climate-induced changes in soil carbon pools

O. Hararuk et al.

[Title Page](#)

[Abstract](#)

[Introduction](#)

[Conclusions](#)

[References](#)

[Tables](#)

[Figures](#)

◀

▶

◀

▶

[Back](#)

[Close](#)

[Full Screen / Esc](#)

[Printer-friendly Version](#)

[Interactive Discussion](#)



patterns were mainly determined by stimulation of NPP. Finally, the combined effects of the three climate variables indicated that overall response is highly driven by the combination of CO<sub>2</sub> and precipitation. Under increasing CO<sub>2</sub> and precipitation, we expect stimulation of soil Hg densities due to large-scale increases in soil C densities, plus 5 direct effects of increased precipitation. Under decreasing precipitation and increasing CO<sub>2</sub>, however, our model predicted losses of soil C densities and associated losses in soil Hg. Our simulations strongly indicated that the overall response of climate change on soil C and soil Hg densities is likely to be highly regional.

This study cannot pinpoint the fate or underlying processes that cause losses or 10 increased accumulation of Hg in soils. On regional scales, however, scenarios that result in losses of Hg from soils might increase mobilization of Hg and adversely affect watershed and ecosystem health in these respective regions; conversely, increased soil accumulation of Hg might increase immobilization and sequestration of Hg thereby 15 potentially reducing bioavailability and exposure. On a global scale, increased soil Hg storage might be beneficial in reducing time periods of surface-atmosphere cycling and re-emissions of Hg, reduced atmospheric exposure and global re-distribution; conversely, if significant soil Hg are re-emitted due to global change or ecosystem disturbances, the legacy of past anthropogenic pollution sources will continue to cycle 20 through environmental compartments. Given the enormous global storage pool of Hg in surface soils, further experimental studies that focus on fate of terrestrial Hg are needed.

**Acknowledgements.** We thank Roger Kreidberg for his help with manuscript editing. This study was funded by the US Environmental Protection Agency (US EPA) through a Science-To-Achieve-Results grant (No. R833378).

## Climate-induced changes in soil carbon pools

O. Hararuk et al.

[Title Page](#)

[Abstract](#)

[Introduction](#)

[Conclusions](#)

[References](#)

[Tables](#)

[Figures](#)

◀

▶

◀

▶

[Back](#)

[Close](#)

[Full Screen / Esc](#)

[Printer-friendly Version](#)

[Interactive Discussion](#)



## References

Aastrup, M., Johnson, J., Bringmark, E., Bringmark, I., and Iverfeldt, A.: Occurrence and transport of mercury within a small catchment area, *Water Air Soil Pollut.*, 56, 155–167, doi:10.1007/BF00342269, 1991.

5 Ainsworth, E. A. and Long, S. P.: What have we learned from 15 years of free-air CO<sub>2</sub> enrichment (FACE)? A meta-analytic review of the responses of photosynthesis, canopy properties and plant production to rising CO<sub>2</sub>, *New Phytol.*, 165, 351–372, doi:10.1111/j.1469-8137.2004.01224.x, 2005.

10 Amirbahman, A., Ruck, P. L., Fernandez, I. J., Haines, T. A., and Kahl, J. A.: The Effect of Fire on Mercury Cycling in the Soils of Forested Watersheds: Acadia National Park, Maine, USA, *Water Air Soil Pollut.*, 152, 315–331, doi:10.1023/B:WATE.0000015369.02804.15, 2004.

15 Andersson, A.: Mercury in soils, Elsevier, Amsterdam, 79–112, 1979.

Artaxo, P., Calixto de Campos, R., Fernandes, E. T., Martins, J. V., Xiao, Z., Lindqvist, O., Fernández-Jiménez, M. T., and Maenhaut, W.: Large scale mercury and trace element measurements in the Amazon basin, *Atmos. Environ.*, 34, 4085–4096, doi:10.1016/S1352-2310(00)00106-0, 2000.

20 Bader, M. K. F. and Körner, C.: No overall stimulation of soil respiration under mature deciduous forest trees after 7 years of CO<sub>2</sub> enrichment, *Glob. Change Biol.*, 16, 2830–2843, doi:10.1111/j.1365-2486.2010.02159.x, 2010.

25 Biester, H., Martinez-Cortizas, A., Birkenstock, S., and Kilian, R.: Effect of Peat Decomposition and Mass Loss on Historic Mercury Records in Peat Bogs from Patagonia, *Environ. Sci. Technol.*, 37, 32–39, 10.1021/es025657u, 2003.

Bonan, G. B., Oleson, K. W., Vertenstein, M., Levis, S., Zeng, X., Dai, Y., Dickinson, R. E., and Yang, Z.-L.: The Land Surface Climatology of the Community Land Model Coupled to the NCAR Community Climate Model, *J. Climate*, 3123–3149, doi:10.1175/1520-0442(2002)015<3123:TLSCOT>2.0.CO;2, 2002a.

30 Bonan, G. B., Levis, S., Kergoat, L., and Oleson, K. W.: Landscapes as patches of plant functional types: An integrating concept for climate and ecosystem models, *Global Biogeochem. Cy.*, 16, 1021–1044, doi:10.1029/2000GB001360, 2002b.

Brunke, E., Labuschagne, C., and Slemr, F.: Gaseous mercury emissions from a fire in the Cape Peninsula, South Africa, during January 2000, *Geophys. Res. Lett.*, 28, 1483–1486, doi:10.1029/2000GL012193, 2001.

## Climate-induced changes in soil carbon pools

O. Hararuk et al.

[Title Page](#)

[Abstract](#)

[Introduction](#)

[Conclusions](#)

[References](#)

[Tables](#)

[Figures](#)

◀

▶

◀

▶

[Back](#)

[Close](#)

[Full Screen / Esc](#)

[Printer-friendly Version](#)

[Interactive Discussion](#)



**Climate-induced changes in soil carbon pools**

O. Hararuk et al.

[Title Page](#)[Abstract](#)[Introduction](#)[Conclusions](#)[References](#)[Tables](#)[Figures](#)[◀](#)[▶](#)[◀](#)[▶](#)[Back](#)[Close](#)[Full Screen / Esc](#)[Printer-friendly Version](#)[Interactive Discussion](#)

## Climate-induced changes in soil carbon pools

O. Hararuk et al.

[Title Page](#)[Abstract](#)[Introduction](#)[Conclusions](#)[References](#)[Tables](#)[Figures](#)[◀](#)[▶](#)[◀](#)[▶](#)[Back](#)[Close](#)[Full Screen / Esc](#)[Printer-friendly Version](#)[Interactive Discussion](#)

Emori, S. and Brown, S. J.: Dynamic and thermodynamic changes in mean and extreme precipitation under changed climate, *Geophys. Res. Lett.*, 32, L17706, doi:10.1029/2005GL023272, 2005.

Engle, M. A., Gustin, M. S., Johnson, D. W., Murphy, J. F., Miller, W. W., Walker, R. F., Wright, J., and Markee, M.: Mercury distribution in two Sierran forest and one desert sagebrush steppe ecosystems and the effects of fire, *Sci. Total Environ.*, 367, 222–233, doi:10.1016/j.scitotenv.2005.11.025, 2006.

Erickson, J. A., Gustin, M. S., Lindberg, S. E., Olund, S. E., and Krabbenhoft, D. P.: Assessing the Potential for Re-emission of Mercury Deposited in Precipitation from Arid Soils Using a Stable Isotope, *Environ. Sci. Technol.*, 39, 8001–8007, doi:10.1021/es0505651, 2005.

Erickson, J. A., Gustin, M. S., Xin, M., Weisberg, P. J., and Fernandez, G. C. J.: Air-soil exchange of mercury from background soils in the United States, *Sci. Total Environ.*, 366, 851–863, doi:10.1016/j.scitotenv.2005.08.019, 2006.

Faïn, X., Obrist, D., Pierce, A., Barth, C., Gustin, M. S., and Boyle, D. P.: Whole-watershed mercury balance at Sagehen Creek, Sierra Nevada, CA, *Geochim. Cosmochim. Acta*, 75, 2379–2392, doi:10.1016/j.gca.2011.01.041, 2011.

Fitzgerald, W. F., Engstrom, D. R., Mason, R. P., and Nater, E. A.: The Case for Atmospheric Mercury Contamination in Remote Areas, *Environ. Sci. Technol.*, 32, 1–7, doi:10.1021/es970284w, 1998.

Friedli, H. R., Radke, L. F., and Lu, J. Y.: Mercury in smoke from biomass fires, *Geophys. Res. Lett.*, 28, 3223–3226, doi:10.1029/2000GL012704, 2001.

Fritsche, J., Obrist, D., Zeeman, M. J., Conen, F., Eugster, W., and Alewell, C.: Elemental mercury fluxes over a sub-alpine grassland determined with two micrometeorological methods, *Atmos. Environ.*, 42, 2922–2933, doi:10.1016/j.atmosenv.2007.12.055, 2008.

Gnamuš, A., Byrne, A. R., and Horvat, M.: Mercury in the Soil-Plant-Deer-Predator Food Chain of a Temperate Forest in Slovenia, *Environ. Sci. Technol.*, 34, 3337–3345, doi:10.1021/es991419w, 2000.

Graydon, J. A., St. Louis, V. L., Hintelmann, H., Lindberg, S. E., Sandilands, K. A., Rudd, J. W. M., Kelly, C. A., Hall, B. D., and Mowat, L. D.: Long-Term Wet and Dry Deposition of Total and Methyl Mercury in the Remote Boreal Ecoregion of Canada, *Environ. Sci. Technol.*, 42, 8345–8351, doi:10.1021/es01056j, 2008a.

Graydon, J. A., St. Louis, V. L., Hintelmann, H., Lindberg, S. E., Sandilands, K. A., Rudd, J. W. M., Kelly, C. A., Hall, B. D., and Mowat, L. D.: Long-Term Wet and Dry Deposition of Total

## Climate-induced changes in soil carbon pools

O. Hararuk et al.

[Title Page](#)[Abstract](#)[Introduction](#)[Conclusions](#)[References](#)[Tables](#)[Figures](#)[◀](#)[▶](#)[◀](#)[▶](#)[Back](#)[Close](#)[Full Screen / Esc](#)[Printer-friendly Version](#)[Interactive Discussion](#)

5 Jobbagy, E. G. and Jackson, R. B.: The Vertical Distribution of Soil Organic Carbon and Its Relation to Climate and Vegetation, *Ecol. Appl.*, 10, 423–436, doi:10.1890/1051-0761(2000)010[0423:TVDOSO]2.0.CO;2, 2000.

10 Johnson, D. W., Hungate, B. A., Dijkstra, B., Hymus, G., and Drake, B.: Effects of Elevated Carbon Dioxide on Soils in a Florida Scrub Oak Ecosystem, *J. Environ. Qual.*, 30, 501–507, doi:10.2134/jeq2001.302501x, 2001.

15 Kubiske, M. E. and Pregitzer, K. S.: Effects of elevated CO<sub>2</sub> and light availability on the photosynthetic light response of trees of contrasting shade tolerance, *Tree Physiol.*, 16, 351–358, doi:10.1093/treephys/16.3.351, 1996.

20 Lag, J. and Steinnes, E.: Regional distribution of mercury in humus layers of Norwegian forest soils, *Acta Agr. Scand.*, 28, 393–396, 1978.

25 Lalonde, J. D., Poulain, A. J., and Amyot, M.: The Role of Mercury Redox Reactions in Snow on Snow-to-Air Mercury Transfer, *Environ. Sci. Technol.*, 36, 174–178, doi:10.1021/es010786g, 2001.

30 Lamborg, C. H., Fitzgerald, W. F., Vandal, G. M., and Rolphus, K. R.: Atmospheric mercury in northern Wisconsin: Sources and species, *Water Air Soil Pollut.*, 80, 189–198, doi:10.1007/BF01189667, 1995.

Landis, M. S., Vette, A. F., and Keeler, G. J.: Atmospheric Mercury in the Lake Michigan Basin: Influence of the Chicago/Gary Urban Area, *Environ. Sci. Technol.*, 36, 4508–4517, doi:10.1021/es011216j, 2002.

35 Lichter, J., Barron, S. H., Bevacqua, C. E., Finzi, A. C., Irving, K. F., Stemmler, E. A., and Schlesinger, W. H.: Soil carbon sequestration and turnover in a pine forest after six years of atmospheric CO<sub>2</sub> enrichment, *Ecology*, 86, 1835–1847, doi:10.1890/04-1205, 2005.

40 Lu, X. Y., Cheng, G. W., Xiao, F. P., and Fan, J. H.: Modeling effects of temperature and precipitation on carbon characteristics and GHGs emissions in *Abies* fabric forest of subalpine, *J. Environ. Sci.*, 20, 339–346, doi:10.1016/s1001-0742(08)60053-4, 2008.

45 Luo, Y., Wan, S., Hui, D., and Wallace, L. L.: Acclimatization of soil respiration to warming in a tall grass prairie, *Nature*, 413, 622–625, doi:10.1038/35098065, 2001a.

## Climate-induced changes in soil carbon pools

O. Hararuk et al.

[Title Page](#)

[Abstract](#)

[Introduction](#)

[Conclusions](#)

[References](#)

[Tables](#)

[Figures](#)

◀

▶

◀

▶

[Back](#)

[Close](#)

[Full Screen / Esc](#)

[Printer-friendly Version](#)

[Interactive Discussion](#)



## Climate-induced changes in soil carbon pools

O. Hararuk et al.

25 Luo, Y., Wu, L., Andrews, J., White, L., Matamala, R., Schäfer, K., and Schlesinger, W. H.: Elevated CO<sub>2</sub> differentiates ecosystem carbon processes: deconvolution analysis of Duke forest FACE data, *Ecological Monographs*, 71, 357–376, doi:10.1890/0012-9615(2001)071[0357:ECDECP]2.0.CO;2, 2001b.

5 Luo, Y., Su, B. O., Currie, W. S., Dukes, J. S., Finzi, A., Hartwig, U., Hungate, B., Murtrie, R. E., Oren, R. A. M., Parton, W. J., Pataki, D. E., Shaw, R. M., Zak, D. R., and Field, C. B.: Progressive Nitrogen Limitation of Ecosystem Responses to Rising Atmospheric Carbon Dioxide, *BioScience*, 54, 731–739, doi:10.1641/0006-3568(2004)054[0731:PNLOER]2.0.CO;2, 2004.

10 Luo, Y., Hui, D., and Zhang, D.: Elevated CO<sub>2</sub> stimulates net accumulations of carbon and nitrogen in land ecosystems: a meta-analysis, *Ecology*, 87, 53–63, doi:10.1890/04-1724, 2006.

Lyman, S. N. and Gustin, M. S.: Speciation of atmospheric mercury at two sites in northern Nevada, USA, *Atmos. Environ.*, 42, 927–939, doi:10.1016/j.atmosenv.2007.10.012, 2008.

15 Ma, L. Q., Tan, F., and Harris, W. G.: Concentrations and distributions of eleven metals in Florida soils, *J. Environ. Qual.*, 26, 769–775, doi:10.2134/jeq1997.00472425002600030025x, 1997.

Mason, R. P., Lawson, N. M., and Sullivan, K. A.: The concentration, speciation and sources of mercury in Chesapeake Bay precipitation, *Atmos. Environ.*, 31, 3541–3550, doi:10.1016/S1352-2310(97)00206-9, 1997.

20 Melillo, M.: The coupling of mercury and organic matter in the biogeochemical cycle – towards a mechanistic model for the boreal forest zone, *Water Air Soil Pollut.*, 56, 333–347, doi:10.1007/BF00342281, 1991.

Melillo, J. M., Steudler, P. A., Aber, J. D., Newkirk, K., Lux, H., Bowles, F. P., Catricala, C., Magill, A., Ahrens, T., and Morrisseau, S.: Soil Warming and Carbon-Cycle Feedbacks to the 25 Climate System, *Science*, 298, 2173–2176, doi:10.1126/science.1074153, 2002.

Millhollen, A. G., Obrist, D., and Gustin, M. S.: Mercury accumulation in grass and forb species as a function of atmospheric carbon dioxide concentrations and mercury exposures in air and soil, *Chemosphere*, 65, 889–897, doi:10.1016/j.chemosphere.2006.03.008, 2006.

30 Morel, F. M. M., Kraepiel, A. M. M., and Amyot, M.: The chemical cycle and bioaccumulation of mercury, *Annu. Rev. Ecol. Systema.*, 29, 543–566, doi:10.1146/annurev.ecolsys.29.1.543, 1998.

Mercury Deposition network: <http://nadp.sws.uiuc.edu/lib/data/2010as.pdf>, 2011.

<a href="#">Title Page</a>	
<a href="#">Abstract</a>	<a href="#">Introduction</a>
<a href="#">Conclusions</a>	<a href="#">References</a>
<a href="#">Tables</a>	<a href="#">Figures</a>
<a href="#">◀</a>	<a href="#">▶</a>
<a href="#">◀</a>	<a href="#">▶</a>
<a href="#">Back</a>	<a href="#">Close</a>
<a href="#">Full Screen / Esc</a>	
<a href="#">Printer-friendly Version</a>	
<a href="#">Interactive Discussion</a>	



## Climate-induced changes in soil carbon pools

O. Hararuk et al.

[Title Page](#)[Abstract](#)[Introduction](#)[Conclusions](#)[References](#)[Tables](#)[Figures](#)[◀](#)[▶](#)[◀](#)[▶](#)[Back](#)[Close](#)[Full Screen / Esc](#)[Printer-friendly Version](#)[Interactive Discussion](#)

## Climate-induced changes in soil carbon pools

O. Hararuk et al.

[Title Page](#)[Abstract](#)[Introduction](#)[Conclusions](#)[References](#)[Tables](#)[Figures](#)[◀](#)[▶](#)[◀](#)[▶](#)[Back](#)[Close](#)[Full Screen / Esc](#)[Printer-friendly Version](#)[Interactive Discussion](#)

Obrist, D., Johnson, D. W., and Edmonds, R. L.: Effects of vegetation type on mercury concentrations and pools in two adjacent coniferous and deciduous forests, *Journal of Plant Nutrition and Soil Science*, 175, 68–77, doi:10.1002/jpln.201000415, 2012.

5 Oechel, W. C., Vourlitis, G. L., Hastings, S. J., Zulueta, R. C., Hinzman, L., and Kane, D.: Acclimation of ecosystem CO<sub>2</sub> exchange in the Alaskan Arctic in response to decadal climate warming, *Nature*, 406, 978–981, doi:10.1038/35023137, 2000.

10 Oleson, K. W., Niu, Z.-L., Yang, G.-Y., Lawrence, D. M., Thornton, P. E., Lawrence, P. J., Stockli, R., Dickinson, R. E., Bonan, G. B., Levis, S., Dai, A., and Qian, T.: Improvements to the Community Land Model and their impact on the hydrological cycle, *J. Geophys. Res.*, 113, G01021, doi:10.1029/2007JG000563, 2008.

Oren, R., Ellsworth, D. S., Johnsen, K. H., Phillips, N., Ewers, B. E., Maier, C., Schafer, K. V. R., McCarthy, H., Hendrey, G., McNulty, S. G., and Katul, G. G.: Soil fertility limits carbon sequestration by forest ecosystems in a CO<sub>2</sub>-enriched atmosphere, *Nature*, 411, 469–472, doi:10.1038/35078064, 2001.

15 Parton, W. J., Schimel, D. S., Cole, C. V., and Ojima, D. S.: Analysis of Factors Controlling Soil Organic Matter Levels in Great Plains Grasslands, *Soil Sci. Soc. Am. J.*, 51, 1173–1179, doi:10.2136/sssaj1987.03615995005100050015x, 1987.

20 Pepper, D. A., Del Grosso, S. J., McMurtrie, R. E., and Parton, W. J.: Simulated carbon sink response of shortgrass steppe, tallgrass prairie and forest ecosystems to rising CO<sub>2</sub>, temperature and nitrogen input, *Global Biogeochem. Cy.*, 19, GB1004, doi:10.1029/2004gb002226, 2005.

Pokharel, A. K. and Obrist, D.: Fate of mercury in tree litter during decomposition, *Biogeosciences*, 8, 2507–2521, doi:10.5194/bg-8-2507-2011, 2011.

25 Qian, T., Dai, A., Trenberth, K. E., and Oleson, K. W.: Simulation of global land surface conditions from 1948 to 2004: Part I: Forcing data and evaluations, *J. Hydrometeorol.*, 7, 953–975, doi:10.1175/JHM540.1, 2006.

Randerson, J. T., Thompson, M. V., Conway, T. J., Fung, I. Y., and Field, C. B.: The contribution of terrestrial sources and sinks to trends in the seasonal cycle of atmospheric carbon dioxide, *Global Biogeochem. Cy.*, 4, 535–560, doi:10.1029/97GB02268, 1997.

30 Randerson, J. T., Hoffman, F. M., Thornton, P. E., Mahowald, N. M., Lindsay, K., Lee, Y.-H., Neivison, C. D., Doney, S. C., Bonan, G., Stockli, R., Covey, C., Running, S. W., and Fung, I. Y.: Systematic assessment of terrestrial biogeochemistry in coupled climate-carbon models, *Glob. Change Biol.*, 15, 2462–2484, doi:10.1111/j.1365-2486.2009.01912.x, 2009.

Rea, A. W., Keeler, G. J., and Scherbatskoy, T.: The deposition of mercury in throughfall and litterfall in the Lake Champlain watershed: A short-term study, *Atmos. Environ.*, 30, 3257–3263, doi:10.1016/1352-2310(96)00087-8, 1996.

5 Reich, J. W. and Schlesinger, W. H.: The global carbon dioxide flux in soil respiration and its relationship to vegetation and climate, *Tellus B*, 44, 81–99, doi:10.1034/j.1600-0889.1992.t01-1-00001.x, 1992.

10 Rustad, L. R., Campbell, J., Marion, G., Norby, R., Mitchell, M., Hartley, A., Cornelissen, J., Gurevitch, J., and Gcte-News: A meta-analysis of the response of soil respiration, net nitrogen mineralization, and aboveground plant growth to experimental ecosystem warming, *Oecologia*, 126, 543–562, doi:10.1007/s004420000544, 2001.

Saiz, G., Bird, M. I., Domingues, T., Schrottd, F., Schwarz, M., Feldpausch, T. R., Veenendaal, E., Djagbletey, G., Hien, F., Compaore, H., Diallo, A., and Lloyd, J.: Variation in soil carbon stocks and their determinants across a precipitation gradient in West Africa, *Glob. Change Biol.*, 18, 1670–1683, doi:10.1111/j.1365-2486.2012.02657.x, 2012.

15 Schroeder, W. H. and Munthe, J.: Atmospheric mercury – An overview, *Atmos. Environ.*, 32, 809–822, doi:10.1016/S1352-2310(97)00293-8, 1998.

Schuster, P. F., Krabbenhoft, D. P., Naftz, D. L., Cecil, L. D., Olson, M. L., Dewild, J. F., Susong, D. D., Green, J. R., and Abbott, M. L.: Atmospheric Mercury Deposition during the Last 270 Years? A Glacial Ice Core Record of Natural and Anthropogenic Sources, *Environ. Sci. Technol.*, 36, 2303–2310, doi:10.1021/es0157503, 2002.

20 Shen, W., Reynolds, J. F., and Hui, D.: Responses of dryland soil respiration and soil carbon pool size to abrupt vs. gradual and individual vs. combined changes in soil temperature, precipitation, and atmospheric [CO<sub>2</sub>]: a simulation analysis, *Glob. Change Biol.*, 15, 2274–2294, doi:10.1111/j.1365-2486.2009.01857.x, 2009.

25 Sigler, J. M., Lee, X., and Munger, W.: Emission and Long-Range Transport of Gaseous Mercury from a Large-Scale Canadian Boreal Forest Fire, *Environ. Sci. Technol.*, 37, 4343–4347, doi:10.1021/es026401r, 2003.

30 Skjellberg, U., Xia, K., Bloom, P. R., Nater, E. A., and Bleam, W. F.: Binding of mercury(II) to reduced sulfur in soil organic matter along upland-peat soil transects, *J. Environ. Qual.*, 29, 855–865, doi:10.2134/jeq2000.00472425002900030022x, 2000.

Smith-Downey, N. V., Sunderland, E. M., and Jacob, D. J.: Anthropogenic impacts on global storage and emissions of mercury from terrestrial soils: Insights from a new global model, *J. Geophys. Res.*, 115, G03008, doi:10.1029/2009JG001124, 2010.

## Climate-induced changes in soil carbon pools

O. Hararuk et al.

[Title Page](#)

[Abstract](#)

[Introduction](#)

[Conclusions](#)

[References](#)

[Tables](#)

[Figures](#)

◀

▶

◀

▶

[Back](#)

[Close](#)

[Full Screen / Esc](#)

[Printer-friendly Version](#)

[Interactive Discussion](#)



Stamenkovic, H., Gustin, M. S., Arnone, J. A., Johnson, D. W., Larsen, J. D., and Verburg, P. S.: Atmospheric mercury exchange with a tallgrass prairie ecosystem housed in mesocosms, *Sci. Total Environ.*, 406, 227–238, doi:10.1016/j.scitotenv.2008.07.047, 2008.

5 Streets, D. G., Devane, M. K., Lu, Z., Bond, T. C., Sunderland, E. M., and Jacob, D. J.: All-Time Releases of Mercury to the Atmosphere from Human Activities, *Environ. Sci. Technol.*, 45, 10485–10491, doi:10.1021/es202765m, 2011.

Talmon, Y., Sternberg, M., and Grunzweig, J. M.: Impact of rainfall manipulations and biotic controls on soil respiration in Mediterranean and desert ecosystems along an aridity gradient, *Glob. Change Biol.*, 17, 1108–1118, doi:10.1111/j.1365-2486.2010.02285.x, 2011.

10 Tingey, D. T., Lee, E. H., Waschmann, R., Johnson, M. G., and Rygiewicz, P. T.: Does soil CO<sub>2</sub> efflux acclimatize to elevated temperature and CO<sub>2</sub> during long-term treatment of Douglas-fir seedlings?, *New Phytol.*, 170, 107–118, doi:10.1111/j.1469-8137.2006.01646.x, 2006.

Treseder, K. K., Egerton-Warburton, L. M., Allen, M. F., Cheng, Y., and Oechel, W. C.: Alteration of Soil Carbon Pools and Communities of Mycorrhizal Fungi in Chaparral Exposed to 15 Elevated Carbon Dioxide, *Ecosystems*, 6, 786–796, doi:10.1007/s10021-003-0182-4, 2003.

Turetsky, M. R., Harden, J. W., Friedli, H. R., Flannigan, M., Payne, N., Crock, J., and Radke, L.: Wildfires threaten mercury stocks in northern soils, *Geophys. Res. Lett.*, 33, L16403, doi:10.1029/2005GL025595, 2006.

Ullrich, S. M., Tanton, T. W., and Abdushitova, S. A.: Mercury in the Aquatic Environment: A Review of Factors Affecting Methylation, *Crit. Rev. Env. Sci.Tec.*, 31, 241–293, doi:10.1080/20016491089226, 2001.

20 Wang, H., Ni, J., and Prentice, I.: Sensitivity of potential natural vegetation in China to projected changes in temperature, precipitation and atmospheric CO<sub>2</sub>), *Regional Environmental Change*, 11, 715–727, doi:10.1007/s10113-011-0204-2, 2011.

25 Wang, S. P., Zhou, G. S., Gao, S. H., and Guo, J. P.: Soil organic carbon and labile carbon along a precipitation gradient and their responses to some environmental changes, *Pedosphere*, 15, 676–680, 2005.

Wigley, T.: The pre-industrial carbon dioxide level, *Climatic Change*, 5, 315–320, doi:10.1007/bf02423528, 1983.

30 Wu, Z., Dijkstra, P., Koch, G. W., Peñuelas, J., and Hungate, B. A.: Responses of terrestrial ecosystems to temperature and precipitation change: a meta-analysis of experimental manipulation, *Glob. Change Biol.*, 17, 927–942, doi:10.1111/j.1365-2486.2010.02302.x, 2011.

## Climate-induced changes in soil carbon pools

O. Hararuk et al.

[Title Page](#)

[Abstract](#)

[Introduction](#)

[Conclusions](#)

[References](#)

[Tables](#)

[Figures](#)

◀

▶

◀

▶

[Back](#)

[Close](#)

[Full Screen / Esc](#)

[Printer-friendly Version](#)

[Interactive Discussion](#)



Zhang, X., Zwiers, F. W., Hegerl, G. C., Lambert, F. G., Gillett, N. P., Solomon, S., Stott, P. A., and Nozawa, T.: Detection of human influence on twentieth-century precipitation trends, *Nature*, 448, 461–465, doi:10.1038/nature06025, 2007.

5 Zheng, Z. M., Yu, G. R., Fu, Y. L., Wang, Y. S., Sun, X. M., and Wang, Y. H.: Temperature sensitivity of soil respiration is affected by prevailing climatic conditions and soil organic carbon content: A trans-China based case study, *Soil Biol. Biochem.*, 41, 1531–1540, doi:10.1016/j.soilbio.2009.04.013, 2009.

10 Zhou, G., Wang, Y., and Wang, S.: Responses of grassland ecosystems to precipitation and land use along the Northeast China Transect, *J. Veg. Sci.*, 13, 361–368, doi:10.1111/j.1654-1103.2002.tb02060.x, 2002.

Zhou, T. and Luo, Y.: Spatial patterns of ecosystem carbon residence time and NPP-driven carbon uptake in the conterminous United States, *Global Biogeochem. Cy.*, 22, GB3032, doi:10.1029/2007GB002939, 2008.

15 Zhou, X., Talley, M., and Luo, Y.: Biomass, Litter, and Soil Respiration Along a Precipitation Gradient in Southern Great Plains, USA, *Ecosystems*, 12, 1369–1380, doi:10.1007/s10021-009-9296-7, 2009.

## Climate-induced changes in soil carbon pools

O. Hararuk et al.

[Title Page](#)

[Abstract](#)

[Introduction](#)

[Conclusions](#)

[References](#)

[Tables](#)

[Figures](#)

◀

▶

◀

▶

[Back](#)

[Close](#)

[Full Screen / Esc](#)

[Printer-friendly Version](#)

[Interactive Discussion](#)



## Climate-induced changes in soil carbon pools

O. Hararuk et al.

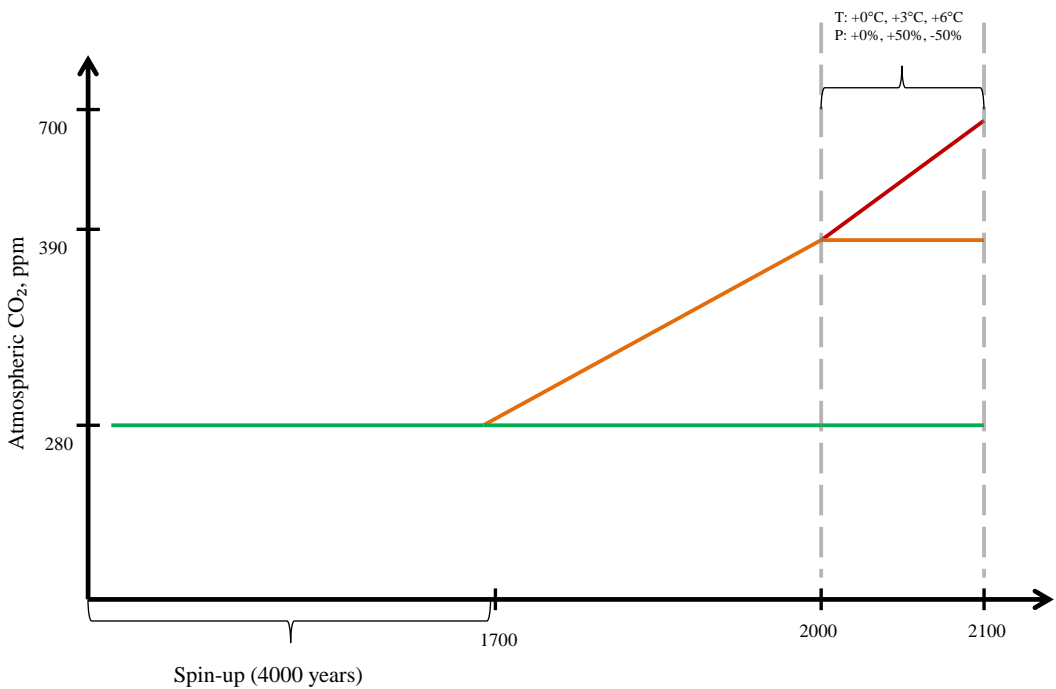


**Fig. 1.** Structure of the model run.

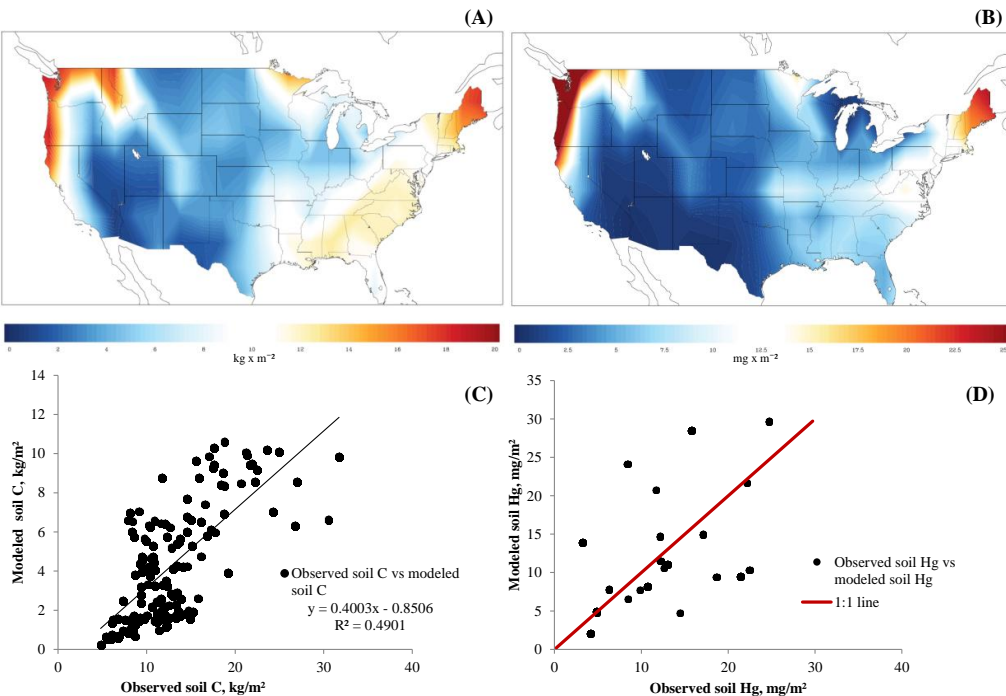


**Fig. 2.** Modeled present day carbon (**A**) and mercury (**B**) densities in the top 40 cm of soils of the contiguous United States. Comparisons of modelled and observed data of soil C and Hg densities (**C** and **D**).

## Climate-induced changes in soil carbon pools

O. Hararuk et al.

[Title Page](#)

[Abstract](#)

[Introduction](#)

[Conclusions](#)

[References](#)

[Tables](#)

[Figures](#)

[◀](#)

[▶](#)

[◀](#)

[▶](#)

[Back](#)

[Close](#)

[Full Screen / Esc](#)

[Printer-friendly Version](#)

[Interactive Discussion](#)

**Climate-induced changes in soil carbon pools**

O. Hararuk et al.

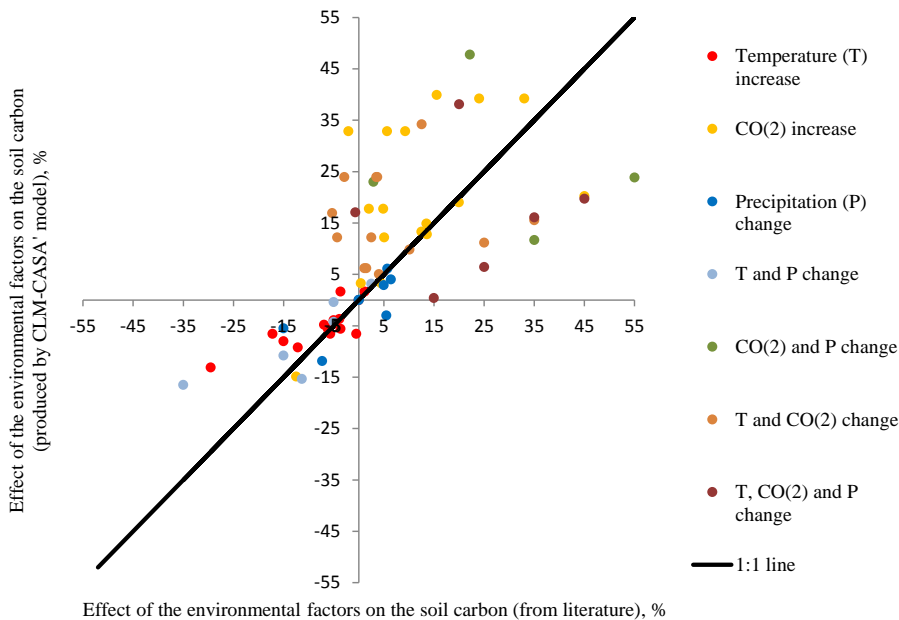


**Fig. 3.** Comparison of change in soil carbon in response to environmental factors reported in the literature to the change obtained in this study.

- [Title Page](#)
- [Abstract](#) [Introduction](#)
- [Conclusions](#) [References](#)
- [Tables](#) [Figures](#)
- [◀](#) [▶](#)
- [◀](#) [▶](#)
- [Back](#) [Close](#)
- [Full Screen / Esc](#)
- [Printer-friendly Version](#)
- [Interactive Discussion](#)

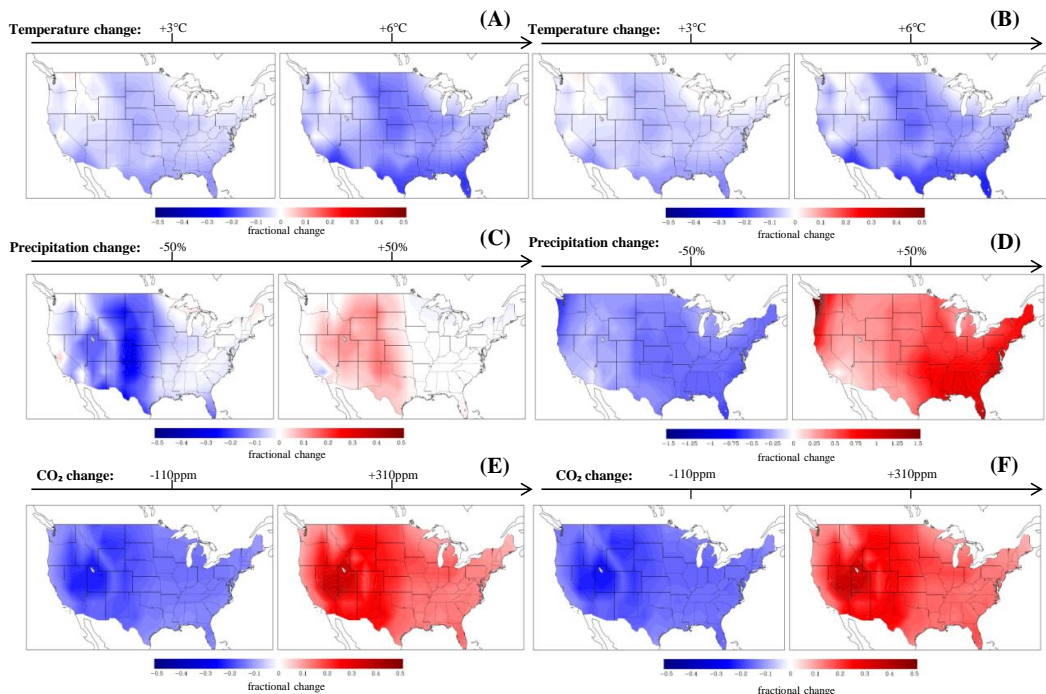


**Fig. 4.** Main effects of temperature, precipitation and CO<sub>2</sub> on top soil carbon (**A, C, E**) and top soil mercury densities (**B, D, F**). The values are expressed as the fractional change of present-day pools.

## Climate-induced changes in soil carbon pools

O. Hararuk et al.

[Title Page](#)

[Abstract](#)

[Introduction](#)

[Conclusions](#)

[References](#)

[Tables](#)

[Figures](#)

◀

▶

◀

▶

[Back](#)

[Close](#)

[Full Screen / Esc](#)

[Printer-friendly Version](#)

[Interactive Discussion](#)

## Climate-induced changes in soil carbon pools

O. Hararuk et al.

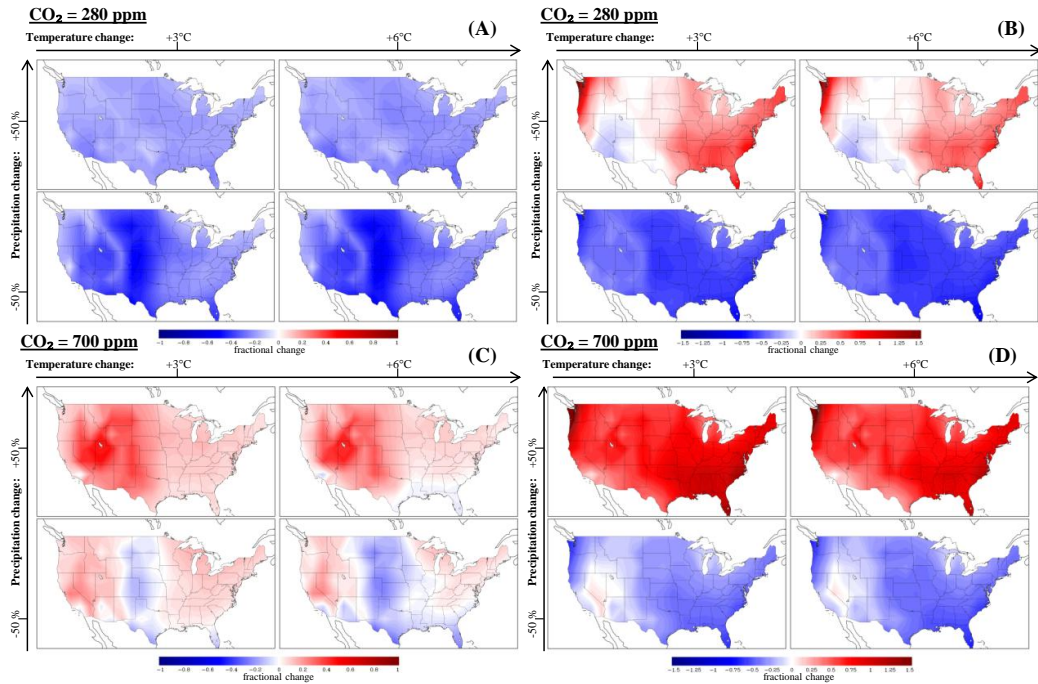


**Fig. 5.** Combined effects of changes in temperature, precipitation, and  $\text{CO}_2$  on soil carbon (**A**, **C**) and soil mercury (**B**, **D**) densities. (**A**) and (**B**) represent the three way interactive effects with  $\text{CO}_2$  concentrations of pre-industrial levels (~110 ppm of present-day), and **C** and **D** show effects with  $\text{CO}_2$  elevated by 420 ppm from present-day levels. Values are expressed as the fractional change of present-day pools.

- [Title Page](#)
- [Abstract](#) [Introduction](#)
- [Conclusions](#) [References](#)
- [Tables](#) [Figures](#)
- [◀](#) [▶](#)
- [◀](#) [▶](#)
- [Back](#) [Close](#)
- [Full Screen / Esc](#)
- [Printer-friendly Version](#)
- [Interactive Discussion](#)